

ey. J

University of California
Ernest O. Lawrence
Radiation Laboratory

PRODUCT ENERGY AND ANGULAR DISTRIBUTIONS FROM
THE REACTION OF N_2^+ WITH ISOTOPIC HYDROGEN MOLECULES

W. R. Gentry, E. A. Gislason, Yuan-tseh Lee,
B. H. Mahan and Chi-wing Tsao

June 1967

RECEIVED
LAWRENCE
RADIATION LABORATORY
SEP 18 1967
LIBRARY AND
DOCUMENTS SECTION

TWO-WEEK LOAN COPY

This is a Library Circulating Copy
which may be borrowed for two weeks.
For a personal retention copy, call
Tech. Info. Division, Ext. 5545

ey. J
UCRL-17674

Submitted to the Disc. Faraday Soc.

UCRL-17674
Preprint

UNIVERSITY OF CALIFORNIA

Lawrence Radiation Laboratory
Berkeley, California

AEC Contract No. W-7405-eng-48

PRODUCT ENERGY AND ANGULAR DISTRIBUTIONS FROM THE REACTION OF

N_2^+ WITH ISOTOPIC HYDROGEN MOLECULES

W. R. Gentry, E. A. Gislason, Yuan-tseh Lee, B. H. Mahan
and Chi-wing Tsao

June, 1967

Product Energy and Angular Distributions from the Reaction of
 N_2^+ with Isotopic Hydrogen Molecules.

By W. R. Gentry,^{*} E. A. Gislason,[†] Yuan-tseh Lee, B. H. Mahan[‡]
and Chi-wing Tsao

^{*} National Science Foundation Predoctoral Fellow.

[†] National Institute of Health Postdoctoral Fellow.

[‡] Alfred P. Sloan Foundation Fellow.

Proofs should be sent to:

Professor Bruce H. Mahan
Department of Chemistry
University of California
Berkeley, California 94720
U.S.A.

Six (6) illustrations are contained in this text.

Short Title: Energy and Angular Distributions.

Abstract

The energy and angular distributions of N_2H^+ and N_2D^+ formed when a beam of N_2^+ passes through a scattering cell containing H_2 , D_2 , or HD have been measured at relative kinetic energies ranging from 2.3 to 11.6 eV. From some experiments, intensity contour maps that show the complete product velocity vector distribution in the center of mass system have been generated. Although backward recoil scattering occurs at all energies, most products are scattered forward in the center of mass system. The shape and position of the forward scattered product peak are largely consistent with the stripping model modified to account for target motion.

The purpose of this work was to investigate the dynamics of the reaction of N_2^+ with H_2 , D_2 , and HD. To do this, a momentum analysed beam of N_2^+ was directed through an isotropic scattering gas, and the energy and angular distributions of products and inelastically scattered reactant ions determined.

Besides its molecular simplicity, the reaction of N_2^+ with the isotopic hydrogens has a number of features that make it attractive for reactive scattering studies. Moderately intense, stable, low energy beams of N_2^+ can be produced without great difficulty. The total reaction cross section is large at low relative energies (100 \AA^2 at 0.1 eV) although it decreases to 1 \AA^2 at 8.5 eV relative energy. The detected product N_2H^+ or N_2D^+ is confined by momentum conservation to a small range of laboratory scattering angles, and the low mass of the product facilitates mass analysis with an instrument of relatively low resolution but high transmission.

The first investigations of these reactions with conventional^{1,2} and then with tandem mass spectrometers^{3,4} served to determine the energy variation of the total reaction cross section. More recently, velocity spectra of ions scattered through small angles have been determined,⁵ and in other experiments^{6,7} energy and some angular distributions of N_2D^+ from the $N_2^+-D_2$ reaction were measured. Despite the considerable attention this reaction has received, more data are needed in order to elucidate the details of the reaction dynamics.

Experimental

The apparatus used will be described in detail in a future publication, but the following general comments will indicate how the experiments were performed. Our instrument consists of a magnetic mass spectrometer for preparation of the primary ion beam, a scattering cell containing the target gas, a 90° spherical electrostatic energy analyser, a quadrupole mass spectrometer and an ion counter. Primary ions from a magnetically confined oscillating electron (50 eV) impact source were extracted and focused on the entrance slit of an unsymmetrical, approximately 60° sector mass spectrometer. Together with its post focusing system, this spectrometer produced an ion beam which had an angular spread of less than 2° full width at half height, and an energy spread of approximately 0.8 eV FWHM.

The primary ions entered a cylindrical scattering cell ($T = 300^\circ\text{K}$) which was located in the center of a large vacuum tank. The gas pressure in the cell was measured directly with an ionization gauge in the H_2 and D_2 experiments. In the experiments with HD, the pressure was monitored by a gauge outside the scattering cell in order to avoid isotopic mixing on the hot filament. When the pressure in the scattering cell was in the usual range of $3-5 \times 10^{-4}$ Torr, the pressure in the surrounding vacuum tank and along the rest of the ion path was only $2-4 \times 10^{-7}$ Torr. Because of this very favorable pressure ratio, corrections due to reactions with the background gas

were always small, and only important for energies and angles very near those of the primary beam.

The exit aperture of the scattering cell, the electrostatic energy analyser, the quadrupole mass spectrometer, and the ion counter were all mounted on a large rotatable lid. By rotating this lid, the exit aperture of the scattering cell as well as the analysing and detecting apparatus could be located within a range of $\pm 55^\circ$ from the primary ion beam. The detector had an angular resolution of 2.5° geometric full width, and an energy resolution of 3% FWHM.

After selecting the desired primary beam energy, the detection mass spectrometer was set to the appropriate mass, and data were collected either by scanning energy at a fixed angle, or scanning the angle at a fixed energy. For each primary beam energy the angular scans were repeated at a series of different analyser energies, and at least one scan of energy was made at zero scattering angle. The result was a set of profiles of the scattered intensity which could either be used individually or combined so as to produce a contour map of scattered intensity. All measurements were normalized to the ion beam intensity, the scattering cell pressure, the transmission band of the energy analyser, and the scattering volume subtended by the detector at the different scattering angles.

Results and Discussion

Twenty-nine experiments were performed in which the distribution of products of reactions of H_2 , D_2 , and HD with N_2^+ at relative energies between 2.3 and 11.6 eV were measured. In six of these experiments enough data were collected to permit construction of contour maps of product intensity. Four of these maps are presented in figs. 1-4, and show the entire angular distribution of reaction products in the center of mass coordinate system. These appear to be the first complete angular distributions reported for any chemical reaction. The most probable velocities of products scattered at 0° and 180° in the center of mass system are given in table 1.

A velocity vector diagram for the reaction of 25 eV N_2^+ with D_2 is shown in fig. 5. Because the thermal velocities of the target molecules are spherically distributed and are mostly quite small compared to the projectile ion velocity, we will take the target molecules to be stationary in the first approximation. The initial relative velocity of collision g is therefore equal to the projectile velocity v_0 , and the initial relative kinetic energy is

$$\frac{\mu g^2}{2} = \frac{1}{2} \frac{M(m_1+m_2)}{M+m_1+m_2} g^2 = \frac{m_1+m_2}{M+m_1+m_2} E_0, \quad (1)$$

where μ is the reduced mass of reactants, M is the projectile mass, m_1 and m_2 are the masses of the hydrogen atoms, and E_0 is

the primary ion laboratory energy. The final relative velocity g' can be calculated from the experimental measurements. Thus the experiments permit the evaluation of the effective exothermicity of the reaction Q , defined by

$$\frac{\mu g^2}{2} + Q = \frac{\mu' (g')^2}{2} \quad (2)$$

$$\mu' = \frac{(M+m_1)m_2}{M+m_1+m_2},$$

where μ' is the reduced mass of the products, and m_1 is the mass of the hydrogen atom in the product ion. Q is the net internal energy converted to translational energy, and can be expressed as

$$Q = W - U, \quad (3)$$

where $W = -\Delta E_0^\circ$ is the heat of reaction, and U is the energy which appears as internal excitation of the products. For the reaction we are investigating

$$W(\text{eV}) = -2.5 + D(\text{N}_2 - \text{H}^+). \quad (4)$$

Here $D(\text{N}_2 - \text{H}^+)$ is the unknown dissociation energy of N_2H^+ into a proton and nitrogen molecule. Isotopic substitution introduces variation of less than 0.1 eV in the value of W .

The general features of the reaction dynamics can be discerned from the intensity contour maps shown in figs. 1-4. The scattering is symmetric about the initial relative velocity vector, except for small deviations attributable to instrumental effects. The product intensity is particularly great at small

angles and speeds close to the projectile speed. Such intense forward scattering in the center of mass system is consistent with the findings of Bailey et al.⁶ and Wolfgang and co-workers.⁷ The scattered intensity at angles greater than 90° is small but finite at all energies investigated. This backward scattering has also been found by others.^{6,7}

At the higher collision energies, the angular distribution assumes an interesting crater-like shape. The total scattered intensity decreases as the projectile energy increases, but the intensity loss is particularly rapid at final relative speeds near zero. It is this excavation of intensity near $g' = 0$ that causes the crater-like distribution to appear at high primary ion energies. This behavior is to be expected, since for zero final relative kinetic speed, all the initial relative kinetic energy and the heat of reaction must be accommodated as internal excitation energy of the product ion. When the internal energy exceeds the dissociation energy of N_2H^+ , this ion will not be found in the products. Combination of eqs. 2, 3, and 4 with $g' = 0$ shows that the maximum initial relative energy for which product ions with no final relative kinetic energy can be formed is 2.5 eV, independent of $D(N_2 - H^+)$.

The fact that some product ions with $g' = 0$ are observed at 2.5 eV and higher initial energies is in part a consequence of imperfect energy and angular resolution. For example, in both the low energy experiments with H_2 and D_2 shown in figs. 1 and 2, the initial relative energy was 3.13 eV, high enough so that no intensity should be observed at $g' = 0$. Both contour

maps show appreciable intensity at this point, however, and only in the experiment with H_2 is there any evidence of a shallow intensity minimum. This small difference is a result of the better energy resolution of the primary beam in the experiment with H_2 .

There is another factor that can lead to product intensity near $g' = 0$ even when the initial kinetic energy is quite high. Because of the isotropic velocity distribution of target molecules, the initial relative kinetic energy may be greater or less than the nominal value calculated by assuming a stationary target. Thus for any projectile velocity molecules moving sufficiently rapidly in the direction of the primary beam may react to form a stable product even if the true final relative kinetic energy is zero. Furthermore, products backscattered from collisions in which the true center of mass velocity exceeds the nominal value, and any forward scattered products from collisions with a true center of mass velocity less than the nominal value will contribute intensity in the region of small apparent g' . Therefore, it is not surprising that product intensity near the center of the crater remains appreciable for initial relative energies above 2.5 eV, and does not fall to zero even in the highest energy experiments.

The concentration of product intensity near 0° suggests that the reaction can be described qualitatively as proceeding in large measure by a pickup or stripping mechanism, as was first proposed by Lacmann and Henglein.⁵ In the ideal stripping process, the projectile interacts with only one hydrogen atom,

and transfers no momentum to the other. Consequently, all product ions formed by this process should be found near 0° with a laboratory energy of $[M/(M+m_1)]E_0$. The finite intensity of products which we find at all large center of mass angles demonstrates that the reactions do not proceed exclusively by the ideal stripping process at any energy. This result is not unexpected, since the small impact parameter collisions which can lead to large angle reactive scattering and recoil of the free atom must always occur. There will be no backward reactive scattering only if the reaction probability for small impact parameter collisions is diminished by competition of other inelastic but non-reactive scattering.

As noted by other workers^{5,6} the ideal stripping model is consistent with the most probable velocity of the forward scattered product peak for initial relative energies of 3-6 eV when H_2 and D_2 are the target molecules. For greater initial energies, the most probable product velocity is higher than that predicted from the ideal stripping model with a stationary target. We have found the same results for both isotopic products from HD as well as H_2 and D_2 . Deviations from the ideal, stationary target stripping model are revealed if any product ion is observed at all for initial relative energies much above 6 eV. The model leads to the prediction that the internal excitation energy of the ion product is

$$U = W + \frac{Mm_1}{M+m_1} \frac{g^2}{2},$$

which is greater than the dissociation energy $D(N_2 - H^+)$ for relative energies greater than

$$\frac{\mu g_{\max}^2}{2} = 2.5 \frac{(M+m_1)(m_1+m_2)}{m_1(M+m_1+m_2)} \text{ eV.} \quad (5)$$

These critical initial kinetic energies are given in table 2. In each case significant product intensity was observed for initial kinetic energies well above the critical value.

These observations suggest that either there is a mechanism by which the product ion can recoil in the forward direction, or that because of the distribution of target velocities, the true relative energies involved in the reactive collisions are less than the nominal values.

It is somewhat difficult to imagine how collisions that give recoil strongly peaked in the forward direction can occur. If a relatively long-lived collision complex between N_2^+ and the target were formed and then separated with product recoil, we would expect to observe not only forward scattering but a product distribution that was isotropic, or nearly so, in the center of mass coordinate system. The intensity contour maps show very clearly that this does not happen, and the conjecture of a long-lived collision complex must be rejected. Moreover, the idea that the collision complex should be long-lived for any collision energy is difficult to accept, and is particularly unattractive when the initial relative energy is high.

Forward recoil can also occur through a collision in which the projectile passes a hydrogen molecule which is so oriented that the closest approach to a hydrogen atom occurs during the outgoing leg of the trajectory. Atom transfer with recoil would then give a product scattered through a relatively small angle in the center of mass system. It would seem, however, that this process would favor small but finite rather than zero angle scattering. If it were dominant at high energies, the forward peak should be broadened in angle, and in the extreme be resolved into a bimodal angular distribution. There is no evidence of this effect in the intensity contour maps. A more damaging argument is that orientation of the target nearly parallel to the projectile trajectory occur less frequently than the perpendicular orientations that would give recoil through moderate to large angles. This is very difficult to reconcile with the observed high intensity at zero scattering angle. Thus grazing collisions with recoil do not provide a satisfactory rationalization of the intense forward scattering.

Another way to account for the intensity and velocity of the forward scattering is to note that stable products can be formed by a stripping mechanism at every beam velocity v_0 provided the relative velocity g is less than the critical value given by eq. (5). Thus when v_0 is greater than g_{\max} , products are formed only in collisions with hydrogen molecules moving rapidly in the direction of the beam. Simple kinematic arguments and recognition of the exponentially decreasing

number of hydrogen molecules with increasing energy are enough to show that the only appreciable contribution to the product intensity comes from collisions where the target velocity is very close to $v_0 - g_{\max}$ in the direction of the ion beam.

With this modified stripping model we can understand the concentration of intensity at zero scattering angle, since only target motion in the beam direction can give stable products. It may also explain the approximately exponential decrease in the intensity of the forward peak observed by Lacmann and Henglein⁵ and ourselves, although a more complete analysis of the energy and angular spread of the beam and the effect of detector resolution is needed to verify this conjecture.

A more detailed test of the modified stripping model is possible. Conservation of momentum requires that

$$v_f = \frac{M}{M+m_1} v_0 + \frac{m_1}{M+m_1} v, \quad (6)$$

where v is the usually neglected velocity of the target, v_f is the product velocity, and v_0 is the projectile velocity, all in the laboratory system. At values of v_0 much less than g_{\max} the target velocity can be neglected, and from eq. (6) we get

$$v_0 - v_f = \frac{m_1}{M+m_1} v_0. \quad (7a)$$

For v_0 greater than g_{\max} , we substitute $v_0 - g_{\max}$ for the target velocity and get

$$v_o - v_f = \frac{m_1}{M+m_1} v_{\max} \quad (7b)$$

Figure 6 shows $v_o - v_f$ plotted as a function of v_o for all our data. The results are in satisfactory agreement with eqs. (7a) and (7b) except for the N_2D^+ product at high velocities. The discrepancy at high energies could very well be a result of the finite energy spread of the primary beam, and may also reflect internal motion of the target and some forward recoil contribution.

If the velocity of the forward peak is determined at high projectile energies by the requirement that $U \leq D(N_2 - H^+)$, the value of Q for this peak should be no more negative than -2.5 eV. Our data show an average limiting value of Q of approximately -2.8 eV for forward scattering at high energies. The apparent value of Q is relatively insensitive to target motion, particularly if the final velocity lies near that predicted by the ideal stripping mechanism. Straightforward analysis shows that for 0° scattering, the error in Q made by assuming a stationary target is

$$2[Mv_o - (M+m_1)v_f] v,$$

to first order in the target velocity v . This vanishes for the ideal stripping process. However, the values of Q are very sensitive to small errors in the measurement of ion energy, and therefore the limiting value of -2.8 eV for Q seems in satisfactory agreement with the expected -2.5 eV.

The contour maps show that at the higher energies products that recoil through angles greater than 45° have a velocity relative to the center of mass that is virtually independent of angle, and an intensity that is small, but increases somewhat for angles greater than 90° . The value of Q is nearly independent of scattering angle and is close to -1.8 eV over much of the range of initial energies. A Q value of -1.8 eV is consistent with the formation of stable products. Whereas the forward scattering can be rationalized successfully in terms of the essentially two-particle stripping model, the analysis of the backward scattering requires consideration of at least a three-particle model for the collision. No simple explanation of the Q value and the variation in intensity at large angles is known.

To summarize, it appears that for high projectile energies the translational energy and angular distribution of products of the reactions of N_2^+ with H_2 , D_2 , and HD is determined principally by two factors: the high probability of atom transfer by the stripping process, and the requirement that the internal energy of the product be less than its dissociation energy. It is the latter factor that is responsible for the crater-like product distribution for high projectile energies. The combination of these factors causes the intense forward scattered product peak to appear at velocities higher than those predicted by the ideal stationary target stripping mechanism.

This work was performed under the auspices of the
U. S. Atomic Energy Commission.

Department of Chemistry and Inorganic Materials Research
Division of the Lawrence Radiation Laboratory, University of
California, Berkeley, California.

References

1. D. O. Schissler and D. P. Stevenson, J. Chem. Physics (1956) 24, 926.
2. T. F. Moran and L. Friedman, J. Chem. Physics (1965) 42, 2391.
3. C. F. Giese and W. B. Maier, J. Chem. Physics (1963) 39, 739.
4. B. R. Turner, M. A. Fineman, and R. F. Stebbings, J. Chem. Physics (1965) 42, 4088.
5. K. Lacmann and A. Henglein, Ber Bunsenges. Physk. Chem. (1965) 69, 292.
6. L. D. Doverspike, R. L. Champion, and T. L. Bailey, J. Chem. Physics (1966) 45, 4385.
7. Z. Herman, J. D. Kerstetter, T. L. Rose, and R. Wolfgang, J. Chem. Physics (1967) 46, 2844.

Table 1. Energetic Data for Forward and Backward Scattering.

Expt	E_o (eV)	E_{rel} (eV)	v_o 10^5 cm/sec	$\chi = 0^\circ$		$\chi = 180^\circ$	
				v_f 10^5 cm/sec	$-Q$ (eV)	v_f 10^5 cm/sec	$-Q$ (eV)
<u>D_2, N_2D^+</u>							
186	65.00	8.125	21.18	20.04	2.49	16.90	1.51
187	24.96	3.119	13.12	12.30	1.47	10.69	1.57
188	35.07	4.384	15.56	14.56	2.15	12.54	1.53
189	75.00	9.375	22.75	21.53	2.82	18.13	1.50
190	24.93	3.117	13.12	12.33	1.32	-	-
191	44.95	5.619	17.61	16.50	2.67	14.22	2.11
192	54.86	6.858	19.46	18.34	2.58	15.67	2.30
193	89.84	11.23	24.90	23.62	2.92	19.89	2.30
<u>H_2, N_2H^+</u>							
194	34.89	2.326	15.52	15.00	1.11	-	-
195	84.32	5.621	24.12	23.33	2.62	21.58	1.72
196	70.09	4.673	21.99	21.21	2.57	19.74	1.88
197	110.23	7.349	27.58	26.69	3.29	24.58	1.24
198	133.86	8.924	30.39	29.48	3.33	27.06	1.28
199	47.00	3.133	18.01	17.33	1.89	16.22	1.56
200	121.68	8.112	28.98	28.08	3.34	25.82	1.32
<u>HD, N_2D^+</u>							
207a	44.84	4.339	17.59	16.48	2.65	15.11	1.41
208a	59.84	5.791	20.32	19.14	2.80	17.42	1.63
210a	74.91	7.249	22.74	21.48	2.97	19.48	1.84
211a	89.86	8.697	24.90	23.62	2.59	21.40	2.93
212a	105.36	10.20	26.96	25.61	2.63	23.15	3.17
213a	119.45	11.56	28.71	27.32	2.26	24.61	3.12
214a	35.05	3.392	15.55	14.49	2.48	-	-

(Continued)

Table 1. (Continued)

Expt	E_o (eV)	E_{rel} (eV)	v_o 10^5 cm/sec	$\chi = 0^\circ$		$\chi = 180^\circ$	
				v_f 10^5 cm/sec	$-Q$ (eV)	v_f 10^5 cm/sec	$-Q$ (eV)
<u>HD, N₂H⁺</u>							
207b	44.84	4.339	17.59	16.96	1.66	14.75	1.33
208b	59.84	5.791	20.32	19.61	2.15	17.00	1.53
210b	74.91	7.249	22.74	21.95	2.61	18.94	1.33
211b	89.86	8.697	24.90	24.12	2.53	20.76	1.76
212b	105.36	10.20	26.96	26.19	2.37	22.48	2.03
213b	119.45	11.56	28.71	27.93	2.32	23.94	2.28
214b	35.05	3.392	15.55	14.97	1.46	13.19	1.68

Table 2. Maximum Initial Energies for
Product Stability.

System	$\frac{\mu g^2}{2}(\text{max})(\text{eV})$	$E_0(\text{max})(\text{eV})$
$\text{H}_2\text{-N}_2\text{H}^+$	4.83	72.5
$\text{D}_2\text{-N}_2\text{D}^+$	4.68	37.5
$\text{HD-N}_2\text{H}^+$	7.01	72.5
$\text{HD-N}_2\text{D}^+$	3.63	37.5

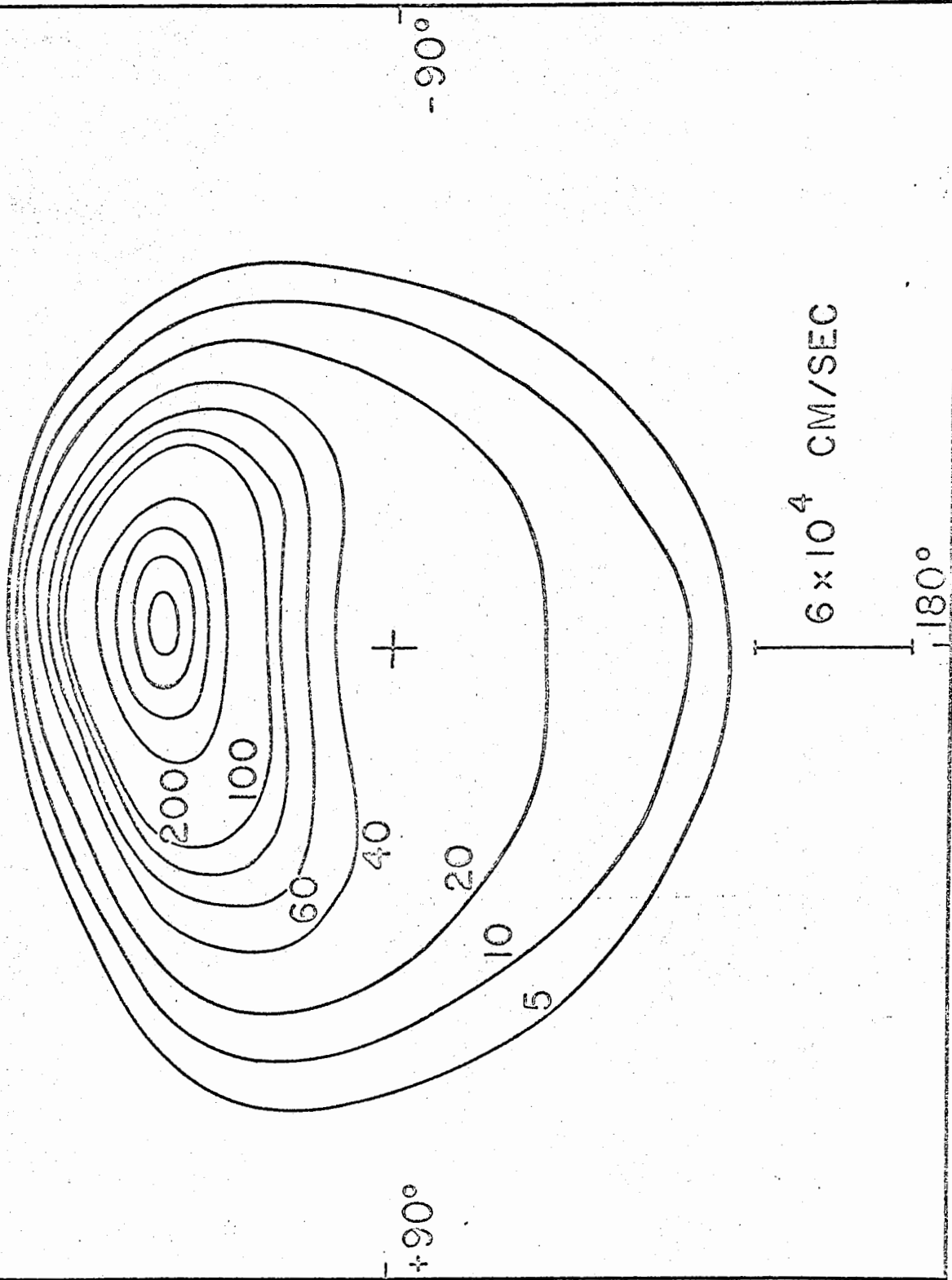


Figure 1. Intensity distribution of N_2D^+ from D_2 plotted in the center of mass polar coordinate system. Intensities at unmarked contours can be found by linear interpolation or extrapolation. Data are from experiment 190 of Table 1, with an initial relative energy of 3.117 eV.

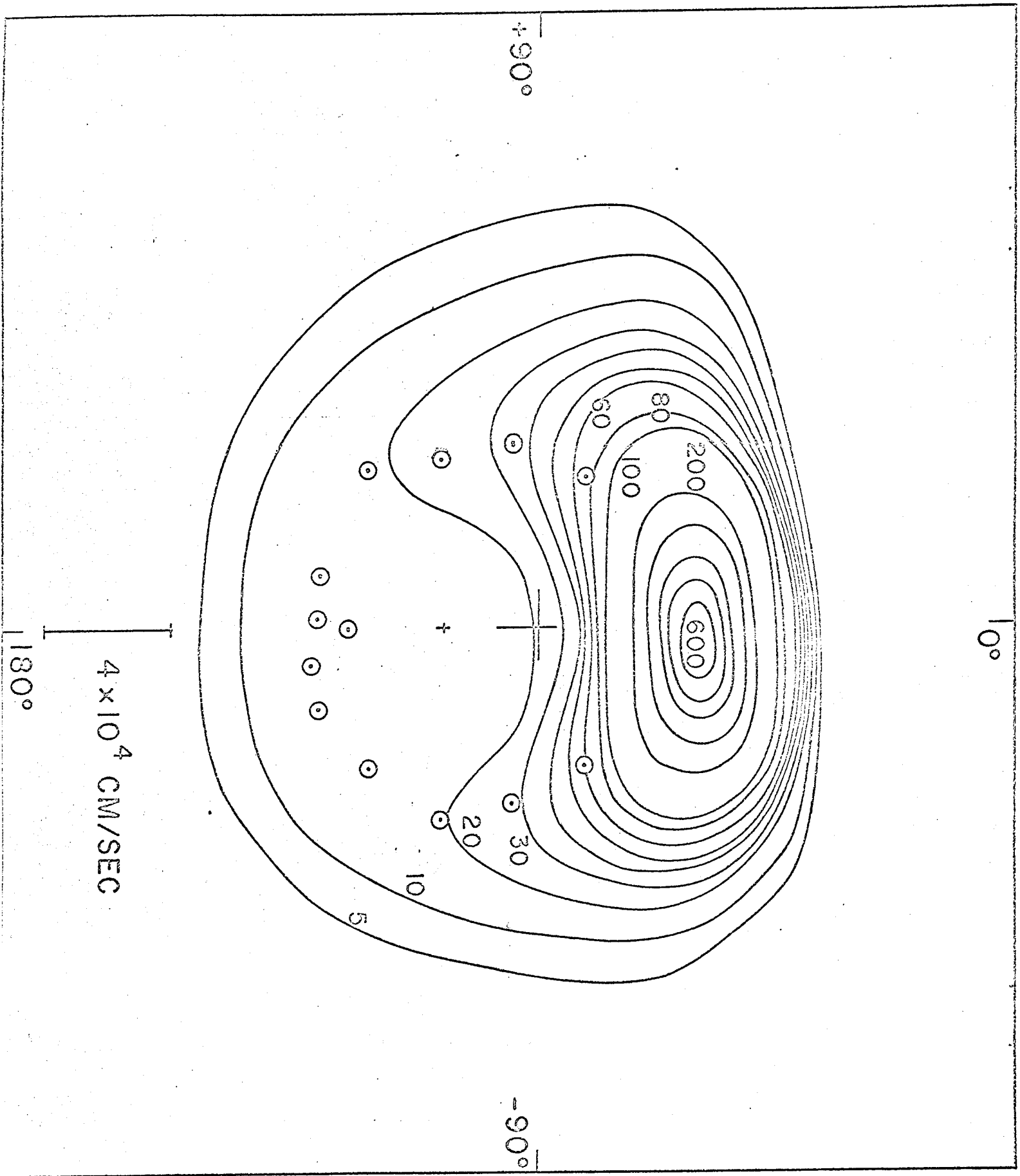


Figure 2. Intensity distribution of N_2H^+ from H_2 plotted in the center of mass polar coordinate system. Circled points give the location of intensity maxima, and the small cross locates a shallow minimum. Data are from experiment 199.

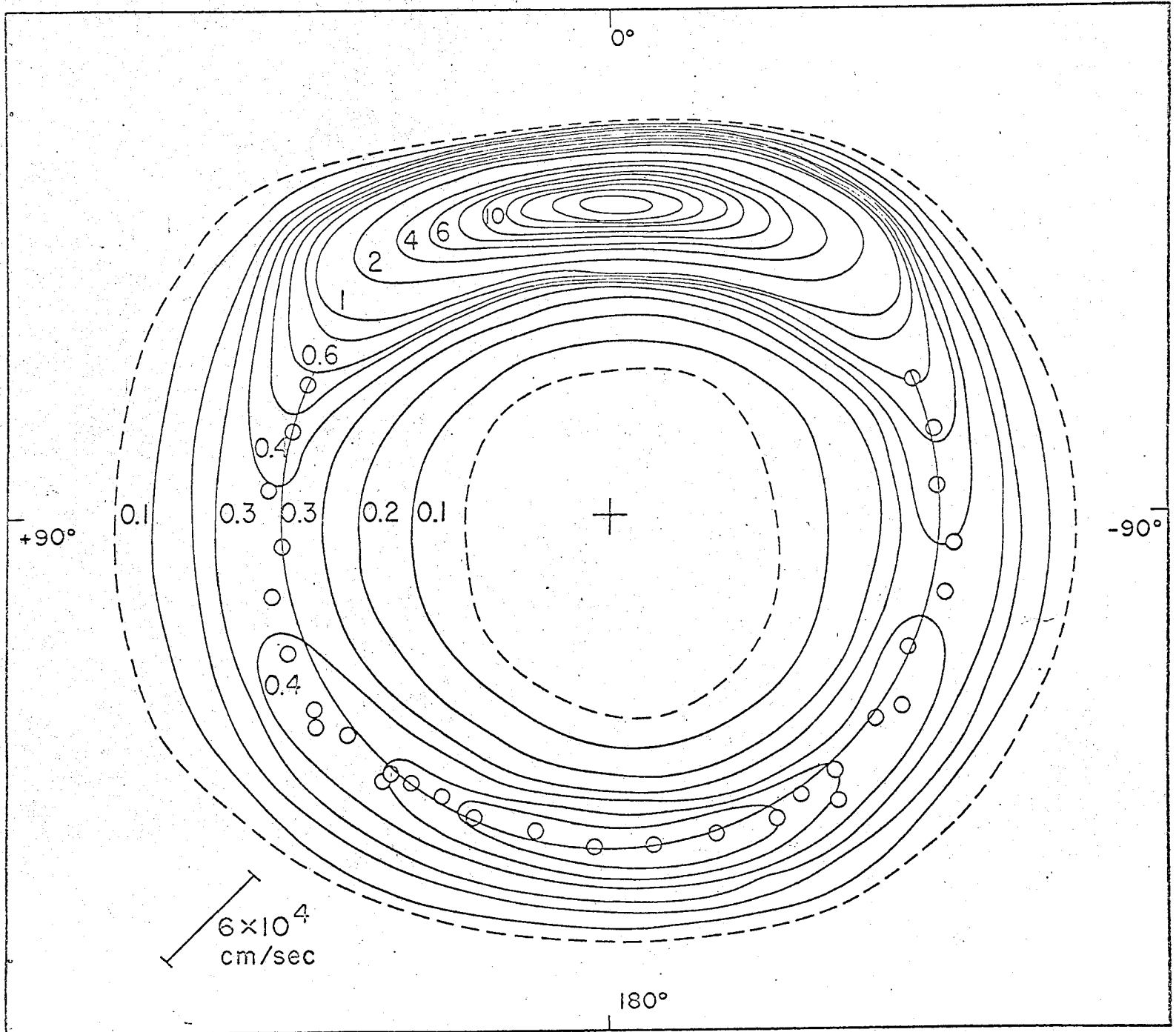


Figure 3. Intensity distribution of N_2D^+ from D_2 . The intensity at $\chi = 0^\circ$ is 18, and at the dotted lines 0.05. Other intensities can be obtained by linear interpolation. The small circles give the location of intensity maxima found from the experimental profiles. The semicircle through the large angle maxima corresponds to $Q = -1.50$ eV. Experiment 186, initial relative energy 8.125 eV.

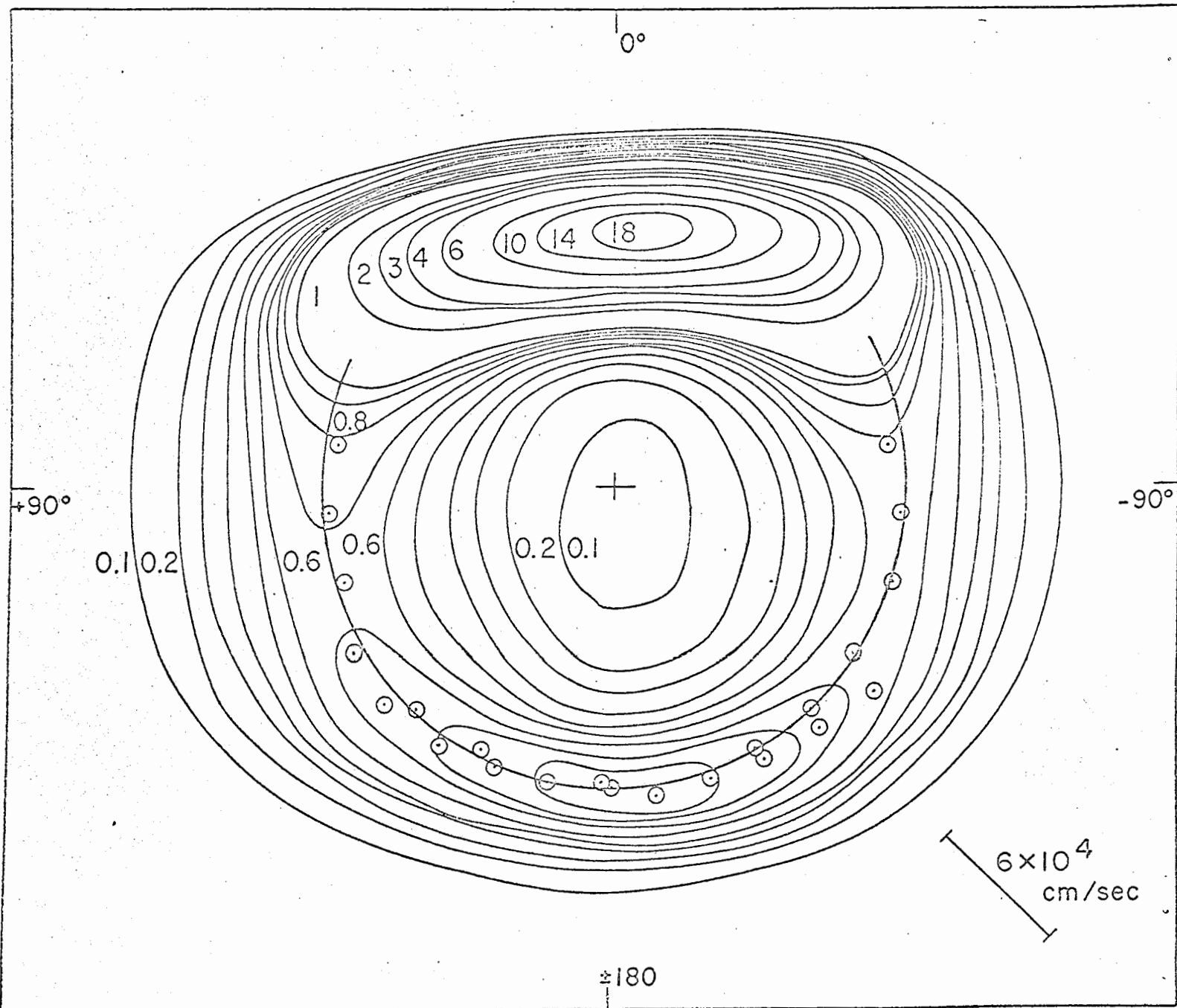


Figure 4. Intensity distribution of N_2H^+ from H_2 in the center of mass system. Data are from experiment 200, with initial relative energy 3.112 eV. The circle through the large angle maxima corresponds to $Q = -1.30$ eV.

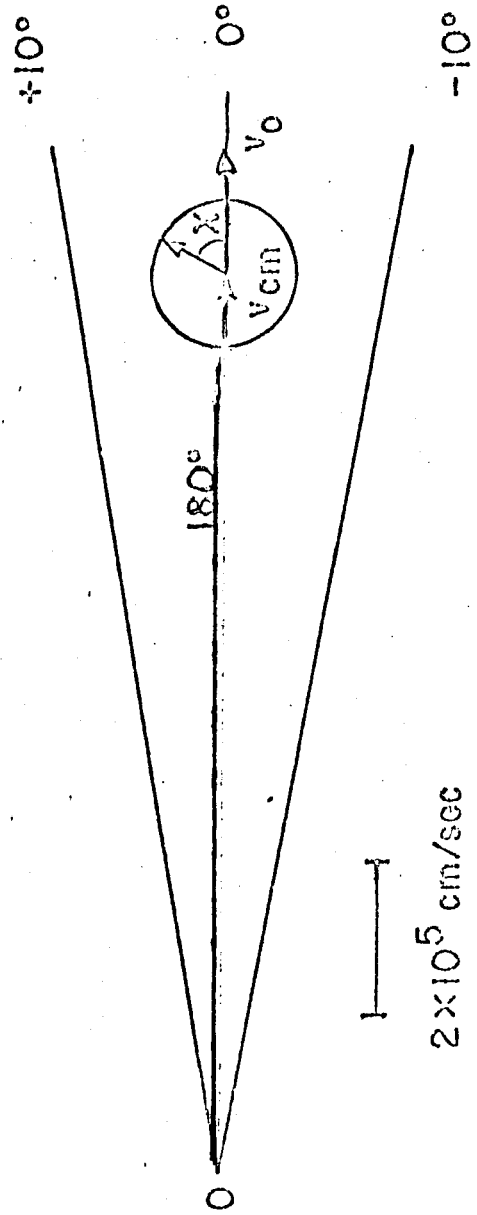


Figure 5. Velocity vector diagram for 25 eV N_2^+ reacting with stationary D_2 . The circle indicates the approximate locus of product intensity maxima.

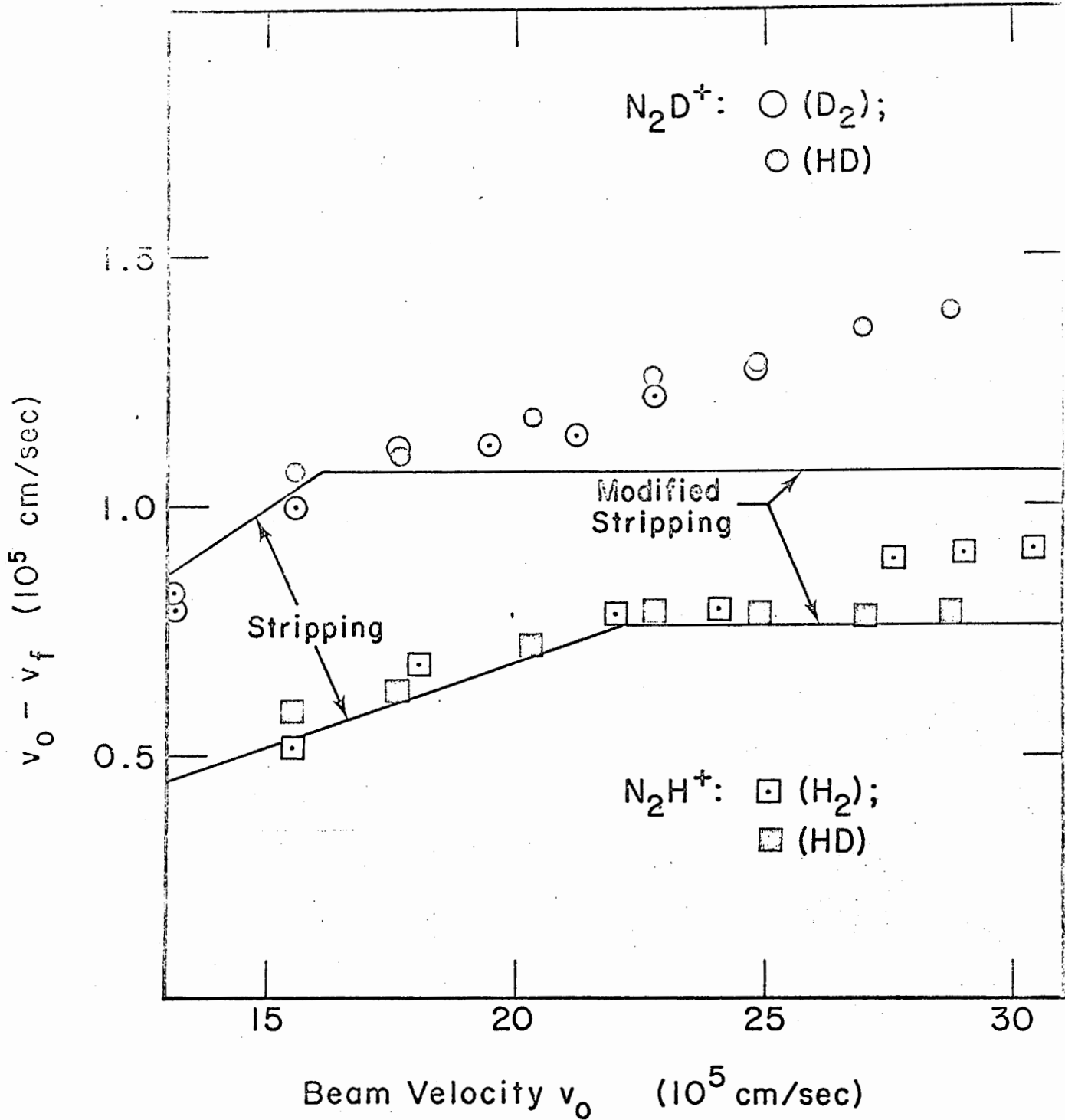


Figure 6. The difference between initial projectile and final product velocities plotted as a function of projectile velocity. The predictions of the stripping and modified stripping models are indicated by the solid lines.

This report was prepared as an account of Government sponsored work. Neither the United States, nor the Commission, nor any person acting on behalf of the Commission:

- A. Makes any warranty or representation, expressed or implied, with respect to the accuracy, completeness, or usefulness of the information contained in this report, or that the use of any information, apparatus, method, or process disclosed in this report may not infringe privately owned rights; or
- B. Assumes any liabilities with respect to the use of, or for damages resulting from the use of any information, apparatus, method, or process disclosed in this report.

As used in the above, "person acting on behalf of the Commission" includes any employee or contractor of the Commission, or employee of such contractor, to the extent that such employee or contractor of the Commission, or employee of such contractor prepares, disseminates, or provides access to, any information pursuant to his employment or contract with the Commission, or his employment with such contractor.